Higher Order Multipole Analysis of Beam Crabbing Mode at 197 MHz for Electron-Ion Collider

Q. Wu

March 2024

Electron-Ion Collider

Brookhaven National Laboratory

U.S. Department of Energy

USDOE Office of Science (SC), Nuclear Physics (NP)

DISCLAIMER

Higher Order Multipole Analysis of Beam Crabbing Mode at 197 MHz for Electron-Ion Collider

Qiong Wu[1], Yun Luo[1], Binping Xiao[1], Subashini De Silva[2], and Zenghai Li[3]

[1]Electron Ion Collider Directorate, Brookhaven National Lab, Upton, NY,11973, USA
[2]OldDominion University, Norfolk, VA, USA
[3]SLAC, Menlo Park, CA, USA

March 18, 2024

Abstract

In the local crabbing scheme for Electron Ion Collider interaction region, beam rotation is initiated by one set of crab cavities at a high beta region with near $90 \deg$ phase advance to the interaction point (IP), and ceased by an identical set of cavities on the symmetrically opposite side. The fundamental mode of all crab cavities is designed to apply a momentum kick to the particle bunches to complete this half cycle of rotation in the horizontal plane, meanwhile the electromagnetic (EM) field can be expanded into a series of harmonics. Despite the lowest dipole mode, higher harmonics cause instabilities during beam operation and loss of particles. We used SimTrack, which is the 6-d symplectic element-by-element tracking code developed at Brookhaven National Laboratory in 2015, to study the threshold of each higher-order harmonic multipolar mode with the criteria of maintaining a dynamic aperture of 6 σ or greater for the Hadron Storage Ring (HSR). In this paper, we showed the threshold for each higher harmonic multipole and their comparison with the multipole strength for the current crab cavity design.

Introduction

In the Electron-Ion Collider's (EIC) baseline configuration, the interaction region features a crossing angle of $25 \, \mathrm{mrad}$ [1]. When compared to the HiLumi LHC project at CERN, which employs a crossing angle of $0.5 \, \mathrm{mrad}$ [2], it becomes evident that this would introduce a significant geometric reduction in

luminosity. The luminosity is calculated to decrease for more than one order of magnitude due to the EIC crossing angle, which would result in an impractically prolonged period for collecting sufficient data for physics experiments.

To recover from this geometric loss, the EIC has adopted the same method used at CERN by implementing a local crabbing system [3] [4]. This local crabbing system involves the installation of a pair of crab cavities positioned symmetrically on either side of the collision point for both the hadron ring and the electron ring. During operation, particle bunches pass through the first set of crab cavities, experiencing a time-dependent horizontal deflection. All crab cavities operate in the same mode such that the integrated crabbing effect imparts a maximum flat kick in opposite directions to the two ends of the bunch, while the center of the bunch remains unaffected.

With this configuration, the bunch initiates betatron oscillations around its central point following its passage through the crab cavity. In the lattice design, the crab cavity system is strategically positioned at a phase advance of $\pm\pi/2$ with respect to the interaction point (IP) at their midpoint. This arrangement ensures that the bunch reaches its maximum rotation angle at the IP.

As depicted in the equation, the voltage is directly proportional to the maximum rotation angle of the bunch. Consequently, the crab cavity's voltage is set to precisely manipulate the bunch rotation angle at the collision point, effectively canceling the geometric angle and restoring a head-on collision configuration.

The EIC crab cavity system comprises fundamental cavities operating at a frequency of 197 MHz and second harmonic cavities at 394 MHz [5] [6]. The fundamental cavities have adopted the RF dipole design from the horizontal crabbing cavity used in the HiLumi LHC project. The primary mode of the cavity is designed for crabbing, and any undesirable higher-order modes can be effectively mitigated using specially designed couplers.

However, it's important to note that the fundamental crabbing mode is not an ideal crabbing field due to boundary conditions. The presence of the deflecting plate at the cavity's center introduces edge effects, together with RF couplers that have broken the symmetry of the cavity, leading to the generation of higher-order multipoles alongside the dipole field. These higher-order multipoles, owing to causality, are all operating in phase. They produce significant nonlinear transverse kicks to the beam, depending on the particles' arrival time at the crab cavity. Such time-dependent kicks may cause nonlinear resonances including the synchro-betatron resonances, therefore impose limitations on the dynamic aperture of the corresponding collider ring.

In this context, we employ tracking simulations through SimTrack [7], which enable us to determine the thresholds for each of these troublesome higher-order multipoles. The insights gained from these thresholds are instrumental in refining the design of the crab cavity, to reduce the amplitudes of these problematic modes to enhance the overall performance of the system.

Multipole Strength from PW theorem

The longitudinal field inside the crab cavity is expressed as $E_s(r, \theta, s)$. It may be expressed in the Fourier form:

$$E_s(r, \theta, s) = \sum_{n=0}^{\infty} \eta_n(s) r^n e^{in\theta}$$

where $\eta_n(s)$ is the Fourier expansion coefficient, which can be calculated for a fixed radius r

$$\eta_n(s) = \frac{1}{r^n} \int_0^{2\pi} E_s(r, \theta, s) e^{-in\theta} d\theta$$

Assuming the particle with speed c does not change trajectory inside the cavity $[0, L]$, the longitudinal momentum change inside the cavity gives:

$$\Delta p_{\parallel} = e^{i\omega z/c + \psi} \left(\frac{q}{c} \int_0^L E_s(r, \theta, s) e^{i\omega s/c} ds \right)$$

From PW theorem,

$$\nabla(\Delta p) = 0$$

$$\frac{\partial}{\partial z}(\Delta p_{\perp}) = -\nabla_{\perp}(\Delta p_{\parallel})$$

Therefore

$$\Delta p_{\perp} = e^{i\omega z/c + \psi} \left(\frac{iq}{\omega} \nabla_{\perp} \int_0^L E_s(r, \theta, s) e^{i\omega s/c} ds \right)$$

Expand the integral inside the parentheses in the Fourier series:

$$A(r, \theta) = \frac{iq}{\omega} \int_0^L E_s(r, \theta, s) e^{i\omega s/c} ds = \sum_{n=1}^{\infty} \frac{r^n}{n} (b_n \cos n\theta + a_n \sin n\theta)$$

Then

$$b_n = \frac{1}{\pi} \int_0^{2\pi} \frac{n}{r^n} A(r, \theta) \cos n\theta d\theta$$

$$a_n = \frac{1}{\pi} \int_0^{2\pi} \frac{n}{r^n} A(r, \theta) \sin n\theta d\theta$$

Then, the momentum change gives:

$$\Delta p_{\parallel} = -e^{i(\omega z/c + \psi)} \frac{i\omega}{c} A(r, \theta)$$

3

From the PW theorem, the transverse momentum change would be:

$$\Delta p_\perp = e^{i(\omega z/c + \psi)} \nabla_\perp A(r, \theta)$$

Re-write the gradient part of the equation $\nabla_\perp A(r, \theta)$:

$$\nabla_\perp A = \frac{\partial A}{\partial r} \hat{r} + \frac{1}{r} \frac{\partial A}{\partial \theta} \hat{\theta}$$

$$\frac{\partial A}{\partial r} = \sum_{n=1}^{\infty} r^{n-1} \left(b_n \cos n\theta + a_n \sin n\theta \right) \equiv \delta p_r$$

$$\frac{1}{r} \frac{\partial A}{\partial \theta} = \sum_{n=1}^{\infty} r^{n-1} \left(-b_n \sin n\theta + a_n \cos n\theta \right) \equiv \delta p_\theta$$

Alternatively, we can write

$$i\delta p_r + \delta p_\theta = \sum_{n=1}^{\infty} r^{n-1} \left(ib_n + a_n \right) e^{in\theta} \tag{1}$$

Therefore we can derive

$$\begin{aligned} i\delta p_x + \delta p_y &= i\delta p_r \cos\theta - i\delta p_\theta \sin\theta + \delta p_r \sin\theta + \delta p_\theta \cos\theta \\ &= \left(i\delta p_r + \delta p_\theta \right) e^{-i\theta} \\ &= \sum_{n=1}^{\infty} r^{n-1} \left(ib_n + a_n \right) e^{i(n-1)\theta} \end{aligned} \tag{2}$$

Combine the equation 1 and equation 2 above:

$$i\delta p_x + \delta p_y = \sum_{n=1}^{\infty} r^{n-1} \left(ib_n + a_n \right) e^{i(n-1)\theta} = \sum_{n=1}^{\infty} \left(ib_n + a_n \right) \left(x + iy \right)^{n-1}$$

The coefficients a_n and b_n correlate with the strength of each order of multipoles.

On the other hand, $\Delta p = \Delta p_\parallel$ is the momentum change due to the multipoles, which is the same as the energy change for $v = c$ particles. The momentum change can be expanded as a summation of terms with coefficients a_n and b_n.

$$\Delta p_\parallel = -e^{i(\omega z/c + \psi)} \frac{i\omega}{c} A(r, \theta) = -e^{i(\omega z/c + \psi)} \frac{i\omega}{c} \sum_{n=1}^{\infty} \frac{r^n}{n} \left(b_n \cos n\theta + a_n \sin n\theta \right)$$

Since

$$\cos n\theta = \frac{e^{in\theta} + e^{-in\theta}}{2}$$

$$\sin n\theta = \frac{e^{in\theta} - e^{-in\theta}}{2}$$

$$r^n e^{in\theta} = (x + iy)^n$$

$$r^n e^{-in\theta} = (x - iy)^n$$

momentum change can be written as

$$\Delta p_{\parallel} = -e^{i(\omega z/c + \psi)}\frac{i\omega}{c}\sum_{n=1}^{\infty}\left\{\frac{b_n}{n}\left[\frac{(x+iy)^n + (x-iy)^n}{2}\right] + \frac{a_n}{n}\left[\frac{(x+iy)^n - (x-iy)^n}{2}\right]\right\} \tag{3}$$

We can derive the multipoles of the crab cavity as well as the momentum change for each n:

Quadrupole $n = 2$

$$\Delta x_2' = \frac{1}{B\rho}\Delta p_x^{(2)} = \frac{1}{B\rho}\delta p_x^{(2)}\cos\left(\frac{\omega z}{c} + \psi\right) = \frac{1}{B\rho}(b_2 x + a_2 y)\cos\left(\frac{\omega z}{c} + \psi\right)$$

$$\Delta y_2' = \frac{1}{B\rho}\Delta p_y^{(2)} = \frac{1}{B\rho}(a_2 x - b_2 y)\cos\left(\frac{\omega z}{c} + \psi\right)$$

$$\Delta p_2 = \frac{1}{B\rho}\Delta p_{\parallel}^{(2)} = \frac{b_2}{B\rho}\frac{\omega}{c}(x^2 - y^2)\sin\left(\frac{\omega z}{c} + \psi\right) + \frac{a_2}{B\rho}\frac{\omega}{c}xy\sin\left(\frac{\omega z}{c} + \psi\right)$$

Sextupole $n = 3$

$$\Delta x_3' = \frac{1}{B\rho}\left[b_3(x^2 - y^2) + 2a_3 xy\right]\cos\left(\frac{\omega z}{c} + \psi\right)$$

$$\Delta y_3' = \frac{1}{B\rho}\left[2b_3 xy + a_3(x^2 - y^2)\right]\cos\left(\frac{\omega z}{c} + \psi\right)$$

$$\Delta p_3 = \frac{b_3}{3B\rho}\frac{\omega}{c}(x^3 - 3xy^2)\sin\left(\frac{\omega z}{c} + \psi\right) + \frac{a_3}{3B\rho}\frac{\omega}{c}\left(3x^2 y - y^3\right)\sin\left(\frac{\omega z}{c} + \psi\right)$$

Octupole $n = 4$

$$\Delta x_4^{'} = \frac{1}{B\rho} \left[b_4(x^3 - 3xy^2) - a_4 \left(y^3 - 3x^2 y \right) \right] \cos \left(\frac{\omega z}{c} + \psi \right)$$

$$\Delta y_4^{'} = \frac{1}{B\rho} \left[b_4(y^3 - 3x^2 y) + a_4 \left(x^3 - 3xy^2 \right) \right] \cos \left(\frac{\omega z}{c} + \psi \right)$$

$$\Delta p_4 = \frac{b_4}{4B\rho} \frac{\omega}{c} (x^4 - 6x^2 y^2 + y^4) \sin \left(\frac{\omega z}{c} + \psi \right)$$
$$+ \frac{a_4}{4B\rho} \frac{\omega}{c} \left(4x^3 y - 4xy^3 \right) \sin \left(\frac{\omega z}{c} + \psi \right)$$

Decapole $n = 5$

$$\Delta x_5^{'} = \frac{1}{B\rho} \left[b_4(x^4 - 6x^2 y^2 + y^4) + a_4 \left(4x^3 y - 4xy^3 \right) \right] \cos \left(\frac{\omega z}{c} + \psi \right)$$

$$\Delta y_4^{'} = \frac{1}{B\rho} \left[b_4(4xy^3 - 4x^3 y) + a_4 \left(x^4 - 6x^2 y^2 + y^4 \right) \right] \cos \left(\frac{\omega z}{c} + \psi \right)$$

$$\Delta p_4 = \frac{b_4}{4B\rho} \frac{\omega}{c} (x^5 - 10x^3 y^2 + 5xy^4) \sin \left(\frac{\omega z}{c} + \psi \right)$$
$$+ \frac{a_4}{4B\rho} \frac{\omega}{c} \left(5x^4 y - 10x^2 y^3 + y^5 \right) \sin \left(\frac{\omega z}{c} + \psi \right)$$

In all equations above, $B\rho$ is the momentum rigidity of the beam, ω is the frequency of the cavity, c is the speed of light, and ψ is the phase advance. All higher-order multipoles are in phase with the main dipole. Each a_n and b_n are the skew and normal multipole coefficient of the $2n$th pole respectively.

Crab Cavity Multipole Effects

The higher-order multipoles of the crab cavity can be computed through fine mesh electric field simulations, as demonstrated in prior studies [8] [9]. These multipoles, arising from the fundamental electric field, introduce transverse deflections to the bunch at each revolution. While the higher-order coefficients ($n > 2$) yield undesired effects in the beam-cavity interaction, they are inevitable due to the asymmetrical structure of the cavity and the coupling of RF auxiliaries into the cavity. Although these high harmonic components are consistently in phase with the crabbing dipole, the electric field may concentrate at locations with small longitudinal offsets from the cavity center, influenced by the asymmetrical structure that induces these components. The additional

Table 1: 197 MHz crab cavity system multipole strength at 33.8 MV.

Type	Vertical Hook FPC	Horizontal Hook FPC	Horizontal Probe FPC
$b_1[T \cdot m]$	0.1120	0.1120	0.1123
$b_2[T]$	0.0030	0.0025	0.0002
$b_3[T/m]$	1.7767	1.7472	1.7591
$b_4[T/m^2]$	0.0256	0.0249	-0.0044
$b_5[T/m^3]$	-93.96	-94.70	-94.01
$b_6[T/m^4]$	45.14	7.496	2.864

transverse kick from these high harmonics can induce instabilities within the bunches as they progress downstream, revealing limitations in the dynamic aperture (DA). Consequently, it is crucial to meticulously evaluate the multipoles with the cavity design and restrict them below a specified threshold to ensure an acceptable dynamic aperture. Accurate fundamental mode field distribution can be exported from the CST Studio [10] simulation with consideration of the meshing convergence from previous studies [8] [9]. The EIC crab cavities are specifically designed to provide a horizontal crabbing kick for collisions, which leads to the skew coefficients a_n being negligible. Therefore, the studies only focus on the dominating normal multipolar components coefficients b_n.

Through a comparison of various design versions of the EIC 197 MHz crab cavity, Table 1, it becomes evident that alterations in multipole strength correlate with specific changes in cavity shape or coupler type, as illustrated in their respective 3D models. While all three designs share the same cavity main body, the distinguishing factor lies in how their fundamental power couplers couple into the cavity field.

The scaling of all multipole coefficients is based on a 33.8 MV crabbing voltage. This voltage represents the total requirement from the 197 MHz crab cavity system on one side of the interaction point, aiming to fully compensate for the 25 mrad crossing angle in the EIC.

Represented by b_1, the primary dipole crab kick, the table highlights that the crab cavity design featuring a Horizontal Probe Fundamental Power Coupler (FPC) achieves a quadrupole b_2 that is an order of magnitude smaller than the other two designs. Moreover, this particular version demonstrates a six-fold reduction in the octupole b_4. The two cavity designs equipped with horizontal FPC couplers exhibit significantly smaller b_6 values when compared to the vertical FPC design. The distinctions in the three FPC coupling schemes contribute to the variance in these even-numbered higher-order multipole strengths. This correlation is further supported by the multipole coefficient plot along the beam axis, depicted in Figure 1. It is essential to recognize that the multipole strengths experienced by the proton beam result from the longitudinal integrated effect of the curves in Figure 1.

Identifying the origin of each higher-order multipole in the cavity design is crucial for the targeted reduction of their strength. Certain multipoles share a
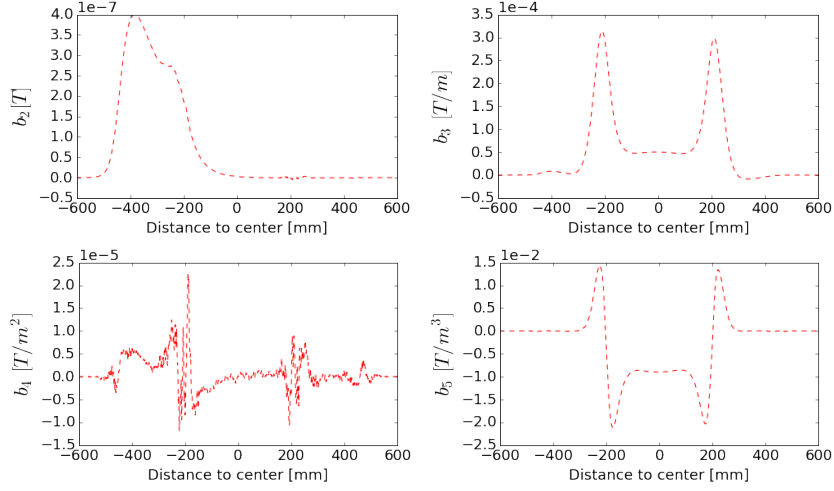
Figure 1: The 197 MHz EIC crab cavity multipole strength with respect to locations in the cavity.

common origin within the design, necessitating that any modifications to the design carefully ensure that all associated multipoles consistently stay below the specified threshold. This precision is essential for maintaining control over the multipole strengths in the design.

Tracking Dynamic Aperture with Crab Cavity Multipoles

We use SimTrack [7] with a parameter scan of the multipolar components of the crabbing mode for Dynamic Aperture (DA) tracking. These studies have assumed the crabbing kick happens at the center of the installation region in the lattice, and all multipoles are treated as a time-dependent thin-length magnet. SimTrack implements exact 6D Hamiltonian and includes nonlinear field errors and optics correction before DA tracking.

SimTrack is a concise C++ code designed for particle tracking in colliders. It employs a 6-dimensional symplectic element-by-element tracking approach, accommodating both 4-dimensional and 6-dimensional weak-strong beam-beam interactions. The code incorporates synchrotron radiation and quantum excitation, along with a linear optics calculation. Additionally, it can fit tune, chromaticity, and orbit corrections. SimTrack serves as a versatile library that allows for expansion or modification. In the context of Dynamic Aperture (DA) analysis, the code tracks twin particles with a separation of 0.025σ. The stability of particle motion at this amplitude is established only when both particles endure over 10^6 turns.

The crossing angle is fixed by the lattice design with constraints from the detector, magnets in the interaction region (IR), facility layout, etc. The deflection provided by the crab cavity is defined by the following equation:

$$V_c = \frac{E_b c \theta_c}{2\omega_c \sqrt{\beta^* \beta_c} \sin \phi_c}$$

Where E_b is the beam energy, c is the speed of light, $/theta_c$ is the full crossing angle, ω_c is the frequency of the crab cavity, β^* and β_c are the beta functions at the IP and crab cavity location respectively, and ϕ_c is the phase advance of the crab cavity.

Based on the existing lattice design, four primary crab cavities operating at a frequency of 197 MHz and two second-harmonic crab cavities at 394 MHz will be installed on each side of the interaction point. These superconducting RF crabbing systems are designed to deliver a linearized crabbing kick, offering total voltages of 33.8 MV and -4.8 MV to the proton beam with an energy of 275 GeV.

To achieve high luminosity for physics experiments, the EIC hadron beam exhibits unequal transverse emittance, with a substantial ratio of 11:1 for horizontal to vertical bunch size. The characterization of the DA involves assessing the mean amplitude, described in terms of the root mean square width of the bunch (σ), at various radial angles across the bunch cross-section. Notably, when the flat beam traverses the round beam pipe with a diameter of 10 cm, the DA imposes more significant constraints on the horizontal direction than the vertical direction. This distribution implies that the limitation of the DA predominantly arises from the horizontal direction. In DA studies, the tracking spans from 0° to 60° to the horizontal plane.

The multipole threshold is established by defining the minimum acceptable DA for the IR, currently set at 6σ. Throughout the tracking process, each multipole consistently interacts with the hadron beam at the same location during each turn. DA is computed after a tracking period comprising 10^6 turns. To understand the DA sensitivity to various multipolar fields, each DA scan is conducted with only one type of crab cavity multipole.

The magnets at IR were set with field errors within the range of $[-10^{-4}, 10^{-4}]$. Each DA is an average of 20 tracking simulations with random IR magnet field errors, and the momentum spread $\delta p/p$ within each bunch is set to 18×10^{-4}.

The Dynamic Aperture (DA) tracking, as depicted in Figure 2, clearly illustrates a reduction in DA as the strength of each multipole increases. In this context, zero degree represents the horizontal x direction, as highlighted in the DA scan for b_3 to b_5 in the Figure.

As demonstrated in Figure 3, a comparison of the DA at various angles to the horizontal direction confirmed the limitation to DA resides within a small angle to the horizontal direction. The envelope of the minimum DA for different azimuthal angles indicated the threshold of the multipole strength. This threshold, established through the 6σ criterion, is considered the maximum value that the cavity design should adhere to in all subsequent multipole threshold studies.
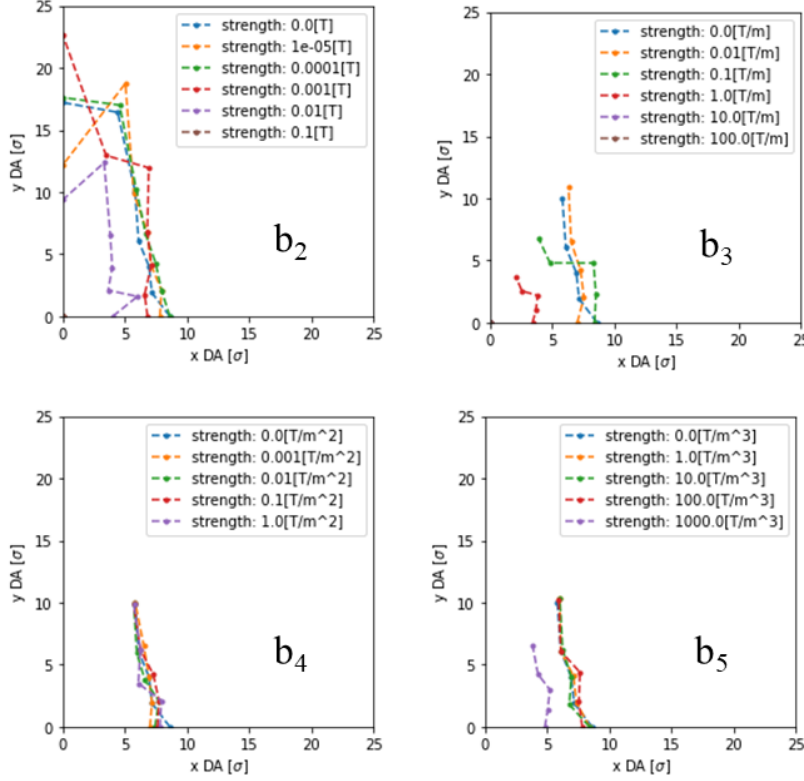
Figure 2: Dynamics aperture scan for multipoles b_2 through b_5 with comparison of various strength

Table 2 summarizes the thresholds for each b_n, as illustrated in Figure 4, ranging from quadrupole to decapole. The table also compared the thresholds with the multipole strengths from the electric probe FPC cavity design. In this design, the sextupole b_3 has exceeded the specified threshold. The b_3 distribution plot in Figure 1 reveals that the primary contributors to the sextupole component are the center deflection plate and the two gaps between the center plate and beam pipes at each end. In contrast to the quadrupole b_2, where the electric field is concentrated solely at the coupler location, the sextupole's electric field is distributed over the effective length of the cavity. Consequently, a viable solution to mitigate the sextupole involves modifying the design of the center deflection plate. The subsequent section discussed cavity design modifications aiming at meeting the sextupole requirement.

The Electron-Ion Collider (EIC) luminosity experiences a 10% increase when local crabbing is applied to the electron beam as well. By considering the electron beam bunch length and the required crabbing voltage, it is feasible for the crabbing system of the Electron Storage Ring (ESR) to operate at the same
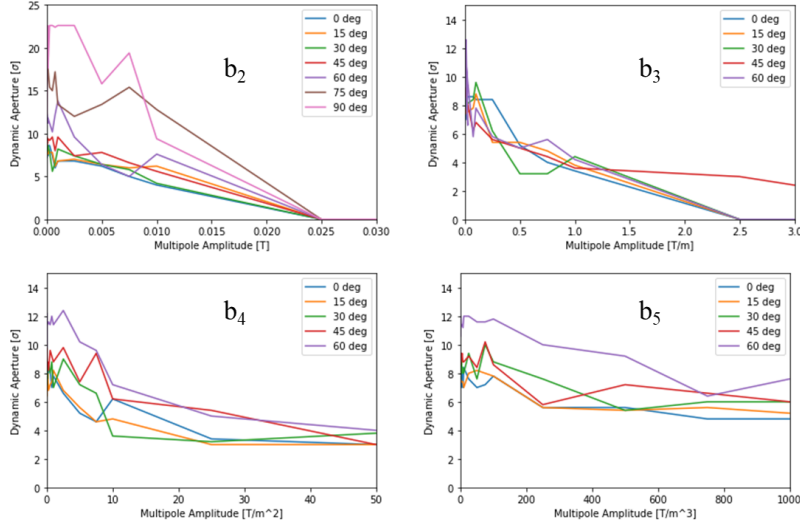
Figure 3: Dynamics aperture scan for multipoles b_2 through b_5 with comparison of various strength

Table 2: 197 MHz crab cavity multipole limitation at 275 GeV proton operation.

	$b_2[T]$	$b_3[T/m]$	$b_4[T/m^2]$	$b_5[T/m^3]$
threshold	0.016	0.32	15.2	-820
Electric Probe FPC design	0.0002	1.7591	-0.0044	-94.01

frequency as the second harmonic of the main hadron ring crab cavities. This approach of using the same system for both purposes eliminates the risks and efforts associated with developing new Superconducting Radio Frequency (SRF) systems.

The addition of second harmonic crab cavities introduces a more linear crabbing kick to the proton bunches which leads to an increase in the dynamic aperture, as illustrated by the effects shown in the Dynamic Aperture (DA) tracking depicted in Figure 5. Notably, the DA threshold for sextupole b_3 increases by 88%, while it more than doubles for decapole b_5. This enhancement in the DA threshold is a significant outcome of employing the second harmonic crab cavities in the system.

Ideally, optimal efficiency in local crabbing is achieved when it occurs at the highest beta function location, with a 180° phase advance between the two sets of crab cavities. However, achieving this ideal scenario proves challenging in the Electron-Ion Collider (EIC) due to the intricate lattice design of IR 6. This complexity arises from accommodating multiple superconducting dipole and quadrupole magnets, along with one set of local crabbing systems within a confined space of 50 meters on each side of the interaction point.
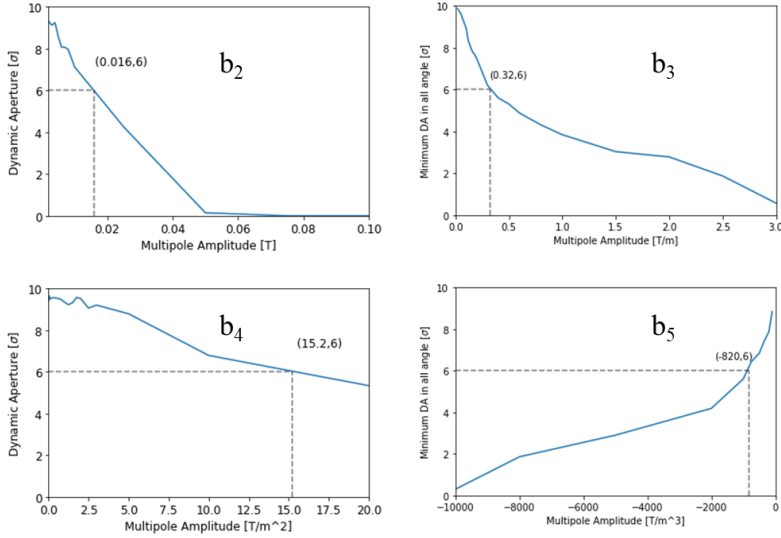
Figure 4: The threshold of each crab cavity multipole corresponding to the minimum dynamic aperture for all angles at 6 σ.

In the current configuration, each set of the local crabbing system comprises 4 main crab cavities at 197 MHz and 2 second harmonic crab cavities at 394 MHz. Furthermore, the IR section lattice must align with the existing Relativistic Heavy Ion Collider (RHIC) ring in the two arcs beyond. The current lattice design has the two crab cavity systems separated by 175°, falling 5° short of the ideal situation. This deviation affects the Dynamic Aperture (DA), as illustrated in Figure 6, where the impact of beam-beam effects and IR errors is also considered.

Crab Cavity Design Improvement

The time dependence of the multipolar electric field generated by the crabbing kick poses a challenge, as conventional magnets in the ring lack the capability to cancel the effect of these crab cavity multipoles. Consequently, the only viable solution to secure an ample DA is establishing a threshold toward multipoles during the cavity design phase. As indicated in Table 2, it is imperative to suppress the sextupole b_3 multipolar component in the cavity design.

The sextupole component can be significantly reduced by introducing curves to the center-deflecting poles of the cavity. Incorporating a slight curvature to the flat region, aligning with the outline of the beam pipe, has proven effective in lowering the sextupole component, as demonstrated in the Hi-Lumi LHC crab cavities. Table 3 compares three different designs. The curved pole design ex-
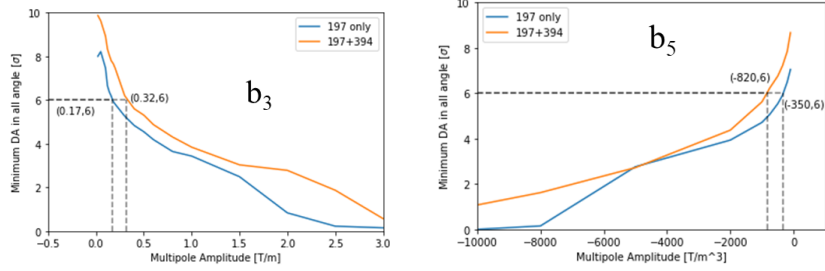
Figure 5: Dynamics aperture comparison of single and double frequency crabbing systems for multipoles b_3 and b_5.
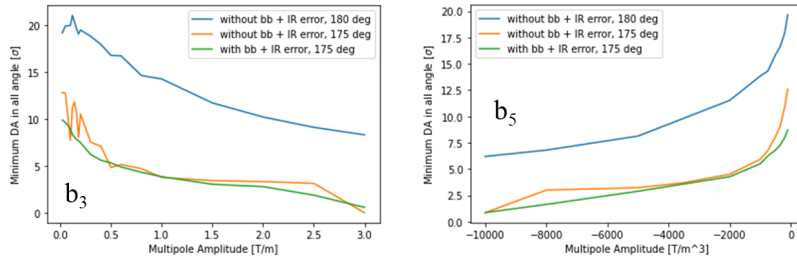

Figure 6: Dynamics aperture comparison of with and without $5°$ offset from ideal crabbing, beam-beam effect, and IR errors for multipoles b_3 and b_5.
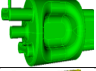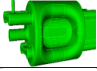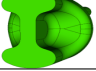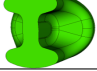
hibited an increase in the decapole strength, which remains below the threshold. To further diminish the decapole component while maintaining the sextupole at a safe level, a short flat strip was added to the center of the curved region, as illustrated in the column labeled "Curve + Flat Pole."

Reducing the multipole strength to ensure dynamic aperture compatibility with crab cavity operation comes with the trade-off of introducing complexity to the cavity design. This heightened complexity, in turn, raises challenges in both the fabrication process and the surface cleaning of the superconducting cavities. Consequently, the ultimate selection of the cavity must approach a balance that accommodates all these considerations.

Summary

The dynamic aperture tracking study revealed that the EIC crab cavity, featuring a flat deflecting pole design, surpasses the sextupole multipole threshold by a factor of five. This condition renders the crab cavity the constraining element in maintaining a dynamic aperture of 6 sigma within the hadron storage ring. Additionally, the limitation to a 175∘ phase advance between the two local crab

Table 3: Multipole comparison for different cavity designs.

	Flat Pole	Curved Pole	Curve + Flat Pole	Multipole Threshold
Cavity				
Pole Surface				
Pole Cross Section				
$b_2[T]$	0.0002	0.0004	0.0004	0.016
$b_3[T/m]$	1.7591	0.055	0.043	0.32
$b_4[T^2/m]$	0.0044	0.011	0.011	15.2
$b_5[T^3/m]$	-94.01	-257	-101.3	-820

cavity sets has significantly narrowed the threshold for the multipoles. Given that the time-dependent momentum kick from these cavities cannot be compensated by the magnets, it is imperative to restrict the multipole components of the cavity by introducing modifications to the cavity design. To address this, the crab cavity deflection pole has been enhanced with curvatures.

The dual-frequency crabbing system for the EIC hadron storage ring comprises the fundamental cavity at 197 MHz and its second harmonic cavity, leveraging the same crab cavity design utilized for the Electron Storage Ring. The threshold for odd multipolar components has been elevated by a factor of 1.9 or more.

References

[1] F. Willeke, and J. Beebe-Wang (editors), "Electron-Ion Collider Conceptual Design Report 2021". United States. https://doi.org/10.2172/1765663

[2] I. Béjar Alonso, O. Brüning, P. Fessia, M. Lamont, L. Rossi, L. Tavian, M. Zerlauth (editors), "High-Luminosity Large Hadron Collider (HL-LHC): Technical Design Report". CERN Yellow Reports: Monographs. CERN, Geneva, 2020.

[3] Q. Wu, "Crab Cavity: Past, Present, and Future of a Challenging Device", presented at the 6th Int. Particle Accelerator Conf. (IPAC'15), Richmond, VA, May 2015, THXB2.

[4] R.Calaga, *et al.*, "First Demonstration of the Use of Crab Cavities on Hadron Beams", *Phys. Rev. Accel. Beams*, 24, 062001(2021)

[5] N. Huque, J. Henry, M. Marchlik, A. Castilla, E. Drachuk, E. F. Daly, S. De Silva, B. Xiao, "Development of a Prototype 197 MHz Crab Cavity for the

Electron-Ion Collider at JLab", presented at the 23rd International Conference on RF Superconductivity, Grad Rapids, MI, August 2023, TUPTB068.

[6] Z. Li, B. Xiao, Q. Wu, W. Xu, J. Delayen, S. De Silva, "EIC 197 MHz Crab Cavity RF Optimization", presented at the 23rd International Conference on RF Superconductivity, Grad Rapids, MI, August 2023, WEPWB051.

[7] Y.Luo, "SimTrack: A Compact C++ Code for Particle Orbit and Spin Tracking in Accelerators", *Nucl. Instrum. and Methods A*, vol.801, pp. 95-103, 2015.

[8] Q. Wu, Y. Luo, B. Xiao, S. De Silva, J. Mitchell, "EIC Crab Cavity Multipole Analysis", presented at the 12th Int. Particle Accelerator Conf. (IPAC'21), Campinas, Brazil, May 2021, WEPAB006.

[9] Q. Wu, Y. Luo, B. Xiao, S. De Silva, Z. Li, "EIC Crab Cavity Multipole Analysis and Their Effects on Dynamic Aperture", presented at the 13th Int. Particle Accelerator Conf. (IPAC'22), Bangkok, Thailand, June 2022, MOPOST009.

[10] CST Microwave Studio Suite 2020, `https://www.3ds.com/products-ser vices/simulia/products/cst-studio-suite/`.